Tuning the self-assembly of lanthanide triple stranded heterobimetallic helicates by ligand design†‡

Thomas B. Jensen, Rosario Scopelliti and Jean-Claude G. Bünzli*

Received 11th October 2007, Accepted 13th November 2007
First published as an Advance Article on the web 4th December 2007
DOI: 10.1039/b715672c

The heterobitopic ligands L^{AB4} and L^{AB5} have been designed and synthesised with the ultimate aim of self-assembling dual-function lanthanide complexes containing either a magnetic and a luminescent probe or two luminescent probes emitting at different wavelengths. They react with lanthanide ions to form complexes of composition $[Ln_2(L^{ABX})_3]^{6+}$ of which three ($X = 4$; Ln = Pr, Nd, Sm) have been isolated and characterised by means of X-ray diffraction. The unit cells contain triple-stranded helicates in which the three ligand strands are wrapped tightly around the two lanthanide ions. In acetonitrile solution the ligands form not only homobimetallic, but also heterobimetallic complexes of composition $[Ln^1Ln^2(L^{ABX})_3]^{6+}$ when reacted with a pair of different lanthanide ions. The yield of heterobimetallic complexes is analyzed in terms of both the difference in ionic radii of the lanthanide ions and of the inherent tendency of the ligands to form high percentages of head-head-head (HHH) helicates in which all three ligand strands are oriented in the same direction with respect to the Ln–Ln vector. The latter is very sensitive to slight modifications of the tridentate coordinating units.

Introduction

The distinctive luminescent properties of trivalent lanthanide ions, including sharp and easily recognisable emissions lines, substantial Stokes' shifts upon ligand excitation, and long lifetimes of the excited states—allowing time-resolved detection for better sensitivity—explain their attractiveness as versatile bioprobes giving off light in the visible and/or near-infrared range.[1–5] Associating two metal centres emitting different colours or having specific luminescent and magnetic properties in a single molecular probe is an attractive way of developing bimodal bioanalyses. While luminescence-detectable contrast agents have been proposed with success,[6–11] dual lanthanide luminescent probes remain largely unexplored, despite the recent development of double lanthanide binding tags in which two identical Ln^{III} ions are bound to a specific peptide.[12]

While several synthetic strategies are available to produce bi- or poly-metallic lanthanide edifices, *e.g.* selective crystallization from a statistical mixture[13] or successive complexation into kinetically inert macrocyclic cavities,[14–16] we are investigating the feasibility of taking advantage of thermodynamically controlled self-assembly processes. Initial experiments involved symmetric hexadentate bitopic ligands, such as L^A (Scheme 1) which forms triple stranded homobimetallic helicates $[Ln_2(L^A)_3]^{6+}$ in acetonitrile.[17,18] The design has been expanded to a whole series of homobitopic ligands L^B,[19] H_2L^C,[20] L^E,[21] L^F,[21] L^G,[22] H_2L^{C2},[23] and H_2L^{C3},[24] the latter two leading to efficient probes for cell imaging. All these ligands afford a 9-coordinate chemical environment for both Ln^{III} ions derived from an idealised D_3 symmetry and similar to the one found for aqua-ions. Increasing the number of tridentate coordination sites gives ligands forming triple-stranded helicates with three[25] or four[26] lanthanide ions.

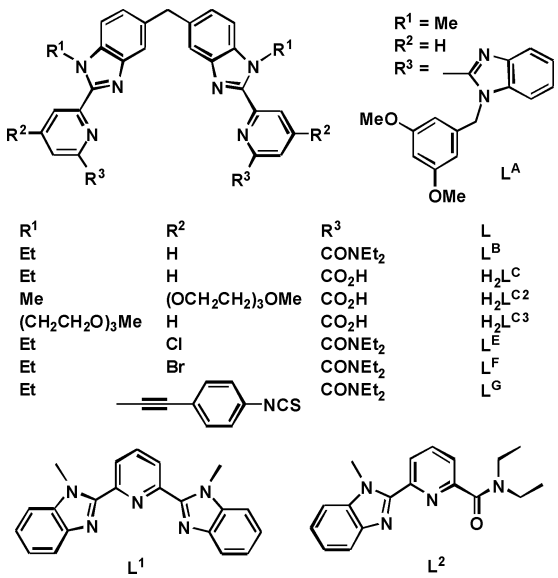

Scheme 1 Structures of symmetrical bitopic and monotopic ligands.

For assembling heterometallic bifunctional edifices, the ligand design is inspired by studies on monometallic $[Ln(L^{1,2})_3]^{3+}$ complexes with tridentate monotopic ligands: L^1 (Scheme 1)[27] has a preference for the larger and mid-size lanthanide ions, a behaviour most likely associated with a supramolecular size-discriminating effect, the coordination cavity being stabilised by interstrand

Laboratory of Lanthanide Supramolecular Chemistry, École Polytechnique Fédérale de Lausanne, BCH 1402, CH-1015, Lausanne, Switzerland. E-mail: jean-claude.bunzli@epfl.ch; Fax: +41 21 69 39 825; Tel: +41 21 69 39 821

† CCDC reference numbers 663485–663487. For crystallographic data in CIF or other electronic format see DOI: 10.1039/b715672c

‡ Electronic supplementary information (ESI) available: Assignment of NMR spectra of ligands, analysis of the coordination polyhedra and aromatic stacking interactions, speciation of homo- and heterobimetallic complexes in solution. See DOI: 10.1039/b715672c

π–π interactions. In contrast, other ligands, exemplified by L^2, form stronger complexes with the smaller lanthanide ions if they display any selectivity at all.[28] Based on this, the heterobitopic ligand L^{AB1} (Scheme 2)[29] was designed to form heterobimetallic complexes of composition $[Ln^1Ln^2(L^{AB1})_3]^{6+}$ when reacted with a heteropair of lanthanide ions, the yield of which depends on the difference in ionic radii of the metal ions. For the heteropair La/Lu, maximising this difference, the yield of the hetero species exceeds 90%. It, however, decreases to about 50% for pairs of lanthanide ions more similar in size.

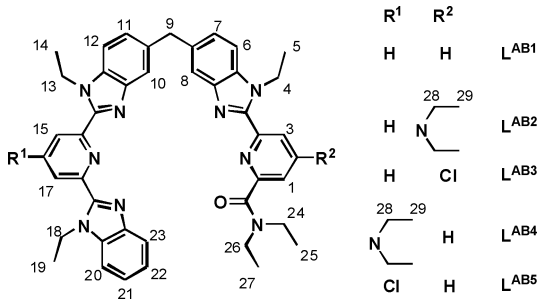

Scheme 2 Structures of heterobitopic ligands with the proton numbering used in NMR assignments.

In the initial heterobitopic ligand L^{AB1} (Scheme 2) the benzimidazole-pyridine-benzimidazole (bpb) moiety, based on ligand L^1, complexes preferentially with the larger Ln^{III} ions when reacted with a pair of different trivalent lanthanide ions. In solution as well as in the solid state the benzimidazole-pyridine-carboxamide (bpa) moiety is always found to bind to the smaller Ln^{III} ion.[29] The electron density of the nitrogen donor atom of the bpa pyridine was modified in ligands L^{AB2} and L^{AB3} by introducing NEt_2 (electron donating) and Cl (electron withdrawing), respectively, in the *para* position of the pyridine.[30] The increased electron density in L^{AB2} was expected to improve the preference of the bpa moiety of the ligand for the smaller and harder Ln^{III} ions, leading to an improved overall selectivity of the ligand; the opposite effect was expected for L^{AB3}. Unexpectedly, the substituents also influenced the yield of HHH (head-head-head) isomer in which the three ligand strands of the $[Ln^1Ln^2(L^{ABX})_3]^{6+}$ complex are pointing in the same direction. This eventually led to lower selectivity of L^{AB2} for heteropairs of Ln^{III} ions, since this ligand preferentially forms the HHT (head-head-tail) isomer, in which one ligand strand is oriented oppositely with respect to the two others. Consequently, we explore here the effect of substitution in the *para* position of the bpb pyridine leading to ligands L^{AB4} and L^{AB5}. The aim of the electron withdrawing Cl in L^{AB5} is to reduce the electron density of the nitrogen donor atom, thus increasing the preference of this complexation unit for larger and softer over smaller and harder Ln^{III} ions. L^{AB4}, with an electron donating NEt_2 group, is designed as a control ligand for which the final selectivity is not expected to be improved.

In this paper, we modify the coordination strength of the bpb moiety, reporting the synthesis of ligands L^{AB4} and L^{AB5} (Scheme 2). The speciation of the resulting helicates is investigated in acetonitrile by means of ^1H NMR. Furthermore, three homobimetallic complexes were crystallised and characterised by X-ray diffraction.

Experimental

Spectroscopic measurements

MS spectra used for the characterization of organic compounds were recorded in CH_3OH or CH_3CN with a Finnigan SSQ-710C spectrometer. 1D ^1H NMR spectra, as well as 2D COSY and ROESY experiments, were performed on a Bruker Avance 400 (400 MHz) spectrometer. Chemical shift values are given in ppm using TMS as reference; J values are given in Hz.

Preparation of ligands

Solvents and starting materials were purchased from Fluka, Acros or Aldrich and used without further purification, unless otherwise stated. Acetonitrile and dichloromethane were distilled from CaH_2; thionyl chloride was distilled from elemental sulfur. Silica gel (Merck 60, 0.04–0.06 mm) was used for preparative column chromatography. Duplicate elemental analyses were performed by Dr H. Eder from the Microchemical Laboratory of the University of Geneva. Compounds **1**,[30] **2**,[31] **5**[21] and **10**[29] were prepared according to published procedures.

Synthesis of compound 3

A solution of **1** (3.18 g; 10.8 mmol), 25 mL of $SOCl_2$ and 5 drops of DMF in 100 mL of dry CH_2Cl_2 was refluxed under N_2 for 2 h. The solvents were evaporated and the residue was dried in a vacuum for 1 h and re-dissolved in 50 mL of dry CH_2Cl_2. A solution of **2** (3.09 g; 18.6 mmol) and 10 mL of NEt_3 in 50 mL of dry CH_2Cl_2 was added dropwise. The solution was refluxed for 1 h, evaporated to dryness and partitioned between 120 mL half saturated aqueous NH_4Cl solution and 120 mL CH_2Cl_2. The aqueous phase was extracted with CH_2Cl_2 (3 × 100 mL) and the combined organic phases were dried over Na_2SO_4, filtered and evaporated to dryness. The crude product was purified on a column (silica gel, CH_2Cl_2–CH_3OH = 100 : 0 → 96 : 4) to give pure **3** (1.79 g, 37%). ^1H NMR ($CDCl_3$): δ 7.94 (dd, 1H, ^3J = 8.3, ^4J = 1.5), 7.46 (td, 1H, ^3J = 7.7, ^4J = 1.5), 7.35 (td, 1H, ^3J = 7.8, ^4J = 1.3), 7.19 (dd, 1H, ^3J = 8.0, ^4J = 1.2), 6.88 (d, 1H, ^4J = 2.7), 6.44 (d, 1H, ^4J = 2.6), 4.35 (sextet, 1H, J = 7.1), 3.55 (sextet, 1H, J = 7.1), 3.41 (sextet, 1H, J = 7.1), 3.32 (q, 4H, J = 7.1), 3.25 (sextet, 1H, J = 7.1), 3.13 (sextet, 1H, J = 7.3), 2.97 (sextet, 1H, J = 7.3), 1.25 (t, 3H, ^3J = 7.2), 1.19 (t, 3H, ^3J = 7.2), 1.11 (t, 6H, ^3J = 7.0), 0.91 (t, 3H, ^3J = 7.0). MS (CH_3CN): m/z: 442.4 ($[M + H]^+$, calcd 442.2).

Synthesis of compound 4

0.99 g of **3** (2.24 mmol), 1.8 g of Fe powder, 5 mL of 25% HCl, 10 mL of H_2O and 45 mL of EtOH was refluxed under N_2 overnight. Excess Fe was filtered off and EtOH was removed by evaporation. The solution was mixed with 100 mL of CH_2Cl_2 and 70 g of $Na_2H_2edta{\cdot}2H_2O$ in 200 mL H_2O. Solid KOH was added up to a pH value of 7. 10 mL of 30% H_2O_2 was added dropwise and the pH was adjusted to 8.5 with solid KOH. After stirring for 30 min the phases were separated and the aqueous phase was extracted with CH_2Cl_2 (4 × 75 mL). The combined organic phases were dried over Na_2SO_4, filtered and evaporated to dryness. The crude product was purified on a column (silica gel, CH_2Cl_2–CH_3OH = 100 : 0 → 97 : 3) to yield **4** (407 mg, 46%). ^1H

NMR ($CDCl_3$): δ 7.82 (dd, 1H, $^3J = 7.0$, $^4J = 2.2$), 7.50 (d, 1H, $^4J = 2.7$), 7.44 (dd, 1H, $^3J = 7.0$, $^4J = 2.0$), 7.31 (td, 1H, $^3J = 7.3$, $^4J = 1.6$), 7.28 (td, 1H, $^3J = 7.2$, $^4J = 1.6$), 6.73 (d, 1H, $^4J = 2.7$), 4.74 (q, 2H, $^3J = 7.1$), 3.58 (q, 2H, $^3J = 7.1$), 3.48 (q, 4H, $^3J = 7.1$), 3.39 (q, 2H, $^3J = 7.1$), 1.44 (t, 3H, $^3J = 7.1$), 1.27 (t, 3H, $^3J = 7.1$), 1.22 (t, 6H, $^3J = 7.1$), 1.08 (t, 3H, $^3J = 7.1$). MS (CH_3CN): m/z: 394.3 ($[M + H]^+$ calcd 394.3).

Synthesis of compound 6

A solution of **5** (1.50 g; 6.96 mmol), 20 mL of $SOCl_2$ and 0.1 mL of DMF in 75 mL of freshly distilled CH_2Cl_2 was refluxed under N_2 for 75 min. After evaporation of the solvent, the residue was dried in a vacuum for 25 min and then re-dissolved in 75 mL of dry CH_2Cl_2. To this solution was added a solution of **2** (1.16 g; 6.96 mmol) and 8 mL of NEt_3 in 75 mL of dry CH_2Cl_2 before refluxing for 60 min. The solvent was evaporated and the residue partitioned between 100 mL of CH_2Cl_2 and 100 mL of half saturated aqueous NH_4Cl. The aqueous phase was extracted with CH_2Cl_2 (2 × 100 mL) and the combined organic extracts were dried over Na_2SO_4, filtered and evaporated to dryness. The product was purified on a column (silica gel, CH_2Cl_2–CH_3OH = 100 : 0 → 98 : 2) to give **6** (2.18 g, 86%). ^{1}H NMR ($CDCl_3$): δ 8.10 (d, 1H, $^4J = 1.8$), 8.04 (dd, 1H, $^3J = 8.2$, $^4J = 1.5$), 7.91 (d, 1H, $^4J = 1.9$), 7.57 (td, 1H, $^3J = 7.7$, $^4J = 1.5$), 7.41 (td, 1H, $^3J = 7.9$, $^4J = 1.5$), 7.35 (dd, 1H, $^3J = 7.8$, $^4J = 1.4$), 4.23 (sextet, $J = 7.1$), 3.80 (s, 3H), 3.72 (sextet, $J = 7.1$), 1.25 (t, 3H, $^3J = 7.2$). MS (CH_3CN): m/z: 364.3 ($[M + H]^+$, calcd 364.1).

Synthesis of compound 7

A mixture of **6** (1.84 g; 5.02 mmol), 6 g of Fe powder, 150 mL of EtOH, 40 mL of H_2O and 30 mL of 25% HCl was refluxed overnight under N_2. Excess Fe was filtered off and EtOH was evaporated on rotavapor. The solution was added to a mixture of 100 mL of CH_2Cl_2 and 40 g of Na_2H_2edta in 150 H_2O and pH was adjusted to 7 with 5 M KOH. After addition of 3 mL of 30% H_2O_2, 5 M KOH was added to pH = 9 and the mixture was stirred for 40 min. After filtration, the phases were separated and the aqueous phase was extracted with CH_2Cl_2 (6 × 100 mL). The combined organic extracts were washed with 150 mL H_2O, dried over Na_2SO_4, filtered and evaporated to dryness. The crude product was purified on a column (silica gel, CH_2Cl_2–CH_3OH = 100 : 0 → 98 : 2) to yield pure **7** (429 g, 26%). ^{1}H NMR ($CDCl_3$): δ 8.68 (d, 1H, $^4J = 1.7$), 8.12 (d, 1H, $^4J = 1.7$), 7.84 (d, 1H, $^3J = 7.9$), 7.49 (d, 1H, $^3J = 7.8$), 7.38 (t, 1H, $^3J = 7.0$), 7.33 (t, 1H, $^3J = 7.2$), 4.92 (q, 2H, $^3J = 7.1$), 4.48 (q, 2H, $^3J = 7.1$), 1.58 (t, 3H, $^3J = 7.1$), 1.46 (t, 3H, $^3J = 7.1$). MS (CH_3CN): m/z: 330.3 ($[M + H]^+$, calcd 330.1).

Synthesis of compound 8

A mixture of **4** (248 mg; 0.63 mmol), 20 g of KOH, 20 mL of EtOH and 30 mL of H_2O was refluxed for 2 d. The EtOH was evaporated and the solution was extracted with CH_2Cl_2 (2 × 50 mL). The pH value was adjusted to 2 with 25% HCl and a white precipitate formed. This was filtered of, washed with aqueous HCl (pH = 2) and dried in vacuum to give **8** (150 mg, 70%). ^{1}H NMR ($CDCl_3$): δ 8.12 (d, 1H, $^3J = 7.3$), 8.00 (s, 1H), 7.61 (d, 1H, $^3J = 7.9$), 7.53 (t, 1H, $^3J = 7.5$), 7.52 (t, 1H, $^3J = 7.4$), 7.47 (s, 1H), 4.90 (q, 2H, $^3J = 7.0$), 3.62 (q, 4H, $^3J = 7.0$), 1.62 (t, 3H, $^3J = 6.9$), 1.28 (t, 3H, $^3J = 7.0$). MS (CH_3CN): m/z: 339.3 ($[M + H]^+$, calcd 339.2).

Synthesis of compound 9

A solution of **7** (429 mg; 1.30 mmol) in 30 mL of 1 M KOH was refluxed overnight. After cooling down, the solution was extracted with 2 × 50 mL CH_2Cl_2 and the pH was adjusted to 1 with 25% HCl. A white precipitate of **9** formed and was filtered off, washed with aqueous HCl (pH = 2) and dried in a vacuum (257 mg, 66%). ^{1}H NMR (DMSO-d_6): δ 8.52 (d, 1H, $^4J = 2.0$), 8.13 (d, 1H, $^4J = 1.9$), 7.75 (d, 1H, $^3J = 8.0$), 7.70 (d, 1H, $^3J = 8.1$), 7.36 (td, 1H, $^3J = 7.6$, $^4J = 1.2$), 7.29 (td, 1H, $^3J = 7.6$, $^4J = 1.2$), 4.89 (q, 2H, $^3J = 7.1$), 1.41 (t, 3H, $^3J = 7.0$). ^{1}H NMR (CD_3OD): δ 8.50 (d, 1H, $^4J = 1.8$), 8.28 (d, 1H, $^4J = 1.8$), 7.75 (m, 2H), 7.50 (t, 1H, $^3J = 7.4$), 7.45 (t, 1H, $^3J = 7.8$), 4.96 (q, 2H, $^3J = 7.2$), 1.57 (t, 3H, $^3J = 7.0$). ^{1}H NMR (CD_3CN): δ 8.58 (d, 1H, $^4J = 1.6$), 8.24 (d, 1H, $^4J = 1.8$), 7.83 (d, 1H, $^3J = 7.8$), 7.71 (d, 1H, $^3J = 8.0$), 7.48 (t, 1H, $^3J = 7.7$), 7.42 (t, 1H, $^3J = 7.5$), 4.87 (q, 2H, $^3J = 7.1$), 1.51 (t, 3H, $^3J = 7.2$). MS (CH_3CN): m/z: 302.4 ($[M + H]^+$ calc. 302.1). Anal. calcd for $C_{15}H_{12}ClN_3O_2 \cdot 1.5H_2O$: C, 54.8; H, 4.6; N, 12.8. Found: C, 55.1; H, 4.1; N, 12.6.

Synthesis of compound 11

A solution of **8** (150 mg; 0.443 mmol), 5 mL of $SOCl_2$ and 0.05 mL of DMF in 50 mL of dry CH_2Cl_2 was refluxed under N_2 for 1 h. The solvent was evaporated and the residue was dried in vacuum for 30 min and re-dissolved in 20 mL of dry CH_2Cl_2. A solution of **10** (550 mg; 1.00 mmol) and 1 mL of NEt_3 in 30 mL of dry CH_2Cl_2 was added dropwise and the reaction mixture was refluxed for 30 min and then left stirring overnight at rt. After evaporation of the solvent the residue was partitioned between 100 mL of CH_2Cl_2 and 100 mL of half saturated aqueous NH_4Cl. The phases were separated and the aqueous phase was extracted with 3 × 30 mL CH_2Cl_2. The combined organic phases were dried over Na_2SO_4, filtered and evaporated to dryness. The residue was purified on a column (silica; CH_2Cl_2–CH_3OH = 100 : 0 → 97 : 3) to give **11** (153 mg, 40%). MS (CH_3CN): m/z: 869.3 ($[M + H]^+$, calcd 869.4); 435.2 ($[M + 2H]^{2+}$, calcd 435.2).

Synthesis of compound 12

A solution of **9** (291 mg; 0.964 mmol), 5 mL of distilled $SOCl_2$ and 0.05 mL of DMF in 50 mL of dry CH_2Cl_2 was refluxed for 80 min. The solvent was evaporated and the residue was dried in a vacuum for 60 min and dissolved in 20 mL of dry CH_2Cl_2. To this solution was added a solution of **10** (1.00 g; 1.82 mmol) and 1.5 mL of distilled NEt_3 in 30 mL of dry CH_2Cl_2. The reaction mixture was refluxed for 2 h and evaporated to dryness. The residue was partitioned between 75 mL of CH_2Cl_2 and 75 mL of half saturated aqueous NH_4Cl solution. After separation of the phases, the aqueous phase was extracted with CH_2Cl_2 (3 × 75 mL) and the combined organic phases were dried over Na_2SO_4, filtered and evaporated to dryness. The residue was purified on column (silica; CH_2Cl_2–CH_3OH = 100 : 0 → 97 : 3) to yield **12** (357 mg, 44%). MS: m/z = 832.3 ($[M + H]^+$, calcd 832.3).

Table 1 Crystallographic data for $[Ln_2(L^{AB4})_3](ClO_4)_6{\cdot}6CH_3CN{\cdot}(CH_3)_3COCH_3$

	Pr_2	Nd_2	Sm_2
Formula	$C_{158}H_{186}Cl_6N_{36}O_{28}Pr_2$	$C_{158}H_{186}Cl_6N_{36}Nd_2O_{28}$	$C_{158}H_{186}Cl_6N_{36}O_{28}Sm_2$
Mol weight	3531.95	3538.61	3550.83
Temp/K	140(2)	100(2)	140(2)
Crystal system	Monoclinic	Monoclinic	Monoclinic
Space group	$P2_1/c$	$P2_1/c$	$P2_1/c$
a/Å	21.2566(15)	21.324(4)	21.3200(16)
b/Å	24.799(2)	24.860(5)	24.6739(11)
c/Å	31.792(2)	31.875(6)	31.934(2)
α/°	90.00	90.00	90.00
β/°	101.684(6)	101.72(3)	102.178(6)
γ/°	90.00	90.00	90.00
V/Å^3	16 412(2)	16 545(6)	16 420.6(18)
F(000)	7320	7328	7344
Z	4	4	4
D_c/Mg m^{-3}	1.429	1.421	1.436
μ(Mo-Kα)/mm^{-1}	0.766	0.798	0.887
Crystal size/mm	0.15 × 0.10 × 0.07	0.13 × 0.10 × 0.06	0.16 × 0.12 × 0.10
Reflections measured	97 229	48 343	96 524
Unique reflections	26 317	14 755	28 163
R(int)	0.2211	0.1600	0.2021
No. of parameters	961	961	961
Constraints	0	0	0
GoF on F^2 [b]	0.714	1.081	0.838
$R1$ [$I > 2\sigma(I)$] [a]	0.0700	0.1046	0.1101
$wR2$ [a]	0.1763	0.2530	0.1858

[a] $R = \Sigma \| F_o | - | F_c \| / \Sigma | F_o |$, $wR2 = [\Sigma [w(F_o^2 - F_c^2)^2] / \Sigma [w(F_o^2)^2]]^{1/2}$. [b] GoF $= [\Sigma [w(F_o^2 - F_c^2)^2] / (n - p)]^{1/2}$.

Synthesis of ligand L^{AB4}

A mixture of **11** (147 mg; 0.169 mmol), 0.6 g of Fe powder, 30 mL of EtOH, 10 mL of H_2O and 5 mL of 25% HCl was refluxed under N_2 for 8 h. The EtOH was evaporated after removal of excess Fe. The solution was mixed with 15 g of $Na_2H_2edta{\cdot}2H2O$, 100 mL of H_2O and 75 mL of CH_2Cl_2 and the pH was adjusted to 7 with solid KOH. Following addition of 4 mL of 30% H_2O_2, solid KOH was added to pH = 8.5 and the mixture was stirred for 2 h. The phases were separated and the aqueous phase was extracted with 3 × 40 mL CH_2Cl_2. The organic extracts were dried over Na_2SO_4, filtered and evaporated to dryness. The crude product was purified on a column (silica; CH_2Cl_2–CH_3OH = 100 : 0 → 96 : 4) to yield pure ligand L^{AB4} (58 mg, 44%). MS (CH_3CN): m/z: 387.4 ([M + 2H]$^{2+}$ calc. 387.2); 773.3 ([M + H]$^+$ calc. 773.4). Anal. calcd for $C_{47}H_{52}N_{10}O{\cdot}H_2O$: C, 73.0; H, 6.8; N, 18.1. Found: C, 73.2; H, 6.7; N, 18.2. See Table S1 (ESI) for the assignment of the ^{1}H NMR spectrum in $CDCl_3$.

Synthesis of ligand L^{AB5}

A mixture of **12** (350 mg; 0.421 mmol), 0.6 g of Fe powder, 30 mL of EtOH, 10 mL of H_2O and 5 mL of 25% HCl was refluxed under N_2 for 7 h. After removal of excess Fe, EtOH was removed by evaporation. The solution was mixed with 16.7 g of $Na_2H_2edta{\cdot}2H_2O$, 150 mL of H_2O and 75 mL of CH_2Cl_2 and the pH value was adjusted to 7 with solid KOH. Following addition of 4 mL of 30% H_2O_2, solid KOH was added to pH = 9 and the solution was stirred for 30 min. The phases were separated and the aqueous phase was extracted with CH_2Cl_2 (3 × 75 mL). The combined organic extracts were dried over Na_2SO_4, filtered and evaporated to dryness. The crude product was purified on column (silica; CH_2Cl_2–CH_3OH = 100 : 0 → 96 : 4) to yield pure ligand L^{AB5} (154 mg, 50%). MS: m/z = 736.3 ([M + H]$^+$, calcd 736.3). Anal. calcd for $C_{43}H_{42}ClN_9O{\cdot}H_2O$: C, 68.5; H, 5.9; N, 16.7. Found: C, 68.8; H, 5.9; N, 16.7. See Table S2 (ESI) for the assignment of the ^{1}H NMR spectrum in $CDCl_3$.

Synthesis of $[Ln_2(L^{ABX})_3](ClO_4)_6$ and $[Ln^1Ln^2(L^{ABX})_3](ClO_4)_6$ (X = 4 or 5) complexes

Partially dehydrated perchlorate salts $Ln(ClO_4)_3{\cdot}xH_2O$ (Ln = La–Lu, $x \approx$ 2–4) were prepared from the corresponding oxides (Rhône-Poulenc, 99.99%) in the usual way.[32] **Caution!** *Perchlorate salts combined with organic ligands are potentially explosive and should be handled in small quantities and with adequate precautions.*[33,34] Stock solutions of $Ln(ClO_4)_3{\cdot}xH_2O$ ($x \approx$ 2–5) in CH_3CN were prepared by weighting. The concentrations of the solutions were determined by complexometric titrations with $Na_2(H_2edta)$ in the presence of urotropine using xylene orange as the indicator.

NMR samples of homobimetallic $[Ln_2(L^{ABX})_3](ClO_4)_6$ complexes were prepared by reacting a weighed amount of L^{ABX} (3–15 mg) dissolved in CH_2Cl_2 with 2/3 equivalents of $Ln(ClO_4)_3{\cdot}xH_2O$ in the form of a CH_3CN solution. After stirring for 1–3 h the solution was evaporated to dryness, the residue was dried in vacuum at 50 °C and re-dissolved in 0.6 mL CD_3CN. Samples of heterobimetallic helicates $[Ln^1Ln^2(L^{ABX})_3](ClO_4)_6$ were prepared in an analogous way using 1/3 equivalent $[Ln^1(ClO_4)_3{\cdot}xH_2O]$ and 1/3 equivalent $[Ln^2(ClO_4)_3{\cdot}xH_2O]$ and stirring the sample overnight before evaporation.

Crystals of homobimetallic triple helicate complexes of L^{AB4} were obtained by reacting 2/3 equivalents of $Ln(ClO_4)_3$ (Ln = Pr, Nd, Sm) with L^{AB4} (5–15 mg) in CH_3CN solution. After evaporation to dryness and drying in vacuum the solid residues

were re-dissolved in a 1 : 1 CH_3CN : CH_3CH_2CN mixture (≈0.5 mL) and precipitated by slow diffusion of *tert*-BuOMe at $T = -18$ °C.

Crystal structure determination of $[Ln_2(L^{AB4})_3](ClO_4)_6 \cdot 6CH_3CN \cdot (CH_3)_3COCH_3$ (Ln = Pr, Nd, Sm)†

Data collections for all compounds have been performed on an Oxford Diffraction Sapphire/KM4 CCD equipped with a kappa geometry goniometer. Data were treated for cell refinement and integration using CrysAlis RED.[35] No absorption correction was applied to the obtained data sets. Structure solutions and refinements have been carried out by SHELXTL.[36] Crystal structures have been refined using the full-matrix on F^2. H atoms have been placed in calculated positions by means of the "riding" model. The entire structures (aside from the metal and chlorine atoms) have been retained as isotropic because the crystals were very weakly diffracting and any attempt to refine them as anisotropic (in combination with suitable restraints) failed. A summary of the general crystal data and refinement parameters is given in Table 1.

Results and discussion

Ligand design, synthesis and properties

The preparation of the two ligands is based on principles developed previously for the synthesis of a rapidly growing family of monotopic[28] as well as homo-[17–23,24] and heterobitopic[29,30,37] ligands (Schemes 1 and 2). The key steps are the formation of the asymmetric secondary amine **10**, which reacts easily with the acid chlorides of **8** or **9** to form **11** and **12**. Closing of the benzimidazole rings by a modified Phillips reaction[38] leads to the targeted ligands in good yields (Scheme 3).

The solution structure of the ligands was investigated by means of ^{1}H-NMR in $CDCl_3$. NOE signals are observed between H24 and H26, H25 and H26, H24 and H27, H25 and H27, H4 and H6, H12 and H13, H18 and H20 (see Scheme 2 for proton numbering). The NOE signals observed between the hydrogen atoms of the bridging methylene group (H9) and all neighbouring benzimidazole hydrogen atoms (H7, H8, H10 and H11) are indicative of free rotation about the methylene group. The absence of signals between pyridine hydrogen atoms (H1, H3, H15 and H17) and ethyl groups (*e.g.* H4, H5, H24 and H25) indicate that the nitrogen atoms of the pyridine groups are oriented in a *transoid* fashion with respect to the other potentially ligating nitrogen atoms. The same kind of structure (free rotation around the central CH_2 group and *transoid* conformation of the pyridine N atoms with respect to the neighbouring pair of potential ligating atoms) has also been observed for the other ligands of this type.

Solid state structure of homobimetallic $[Ln_2(L^{AB4})_3](ClO_4)_6$ helicates

Both L^{AB4} and L^{AB5} react with 2/3 equivalent of Ln^{III} ions to form triple-stranded bimetallic helicates in acetonitrile solution. We were able to isolate crystals of X-ray quality of the three complexes $[Ln_2(L^{AB4})_3](ClO_4)_6 \cdot$solvent (Ln = Pr, Nd, Sm) (Table 1). The three compounds are isostructural and the unit cell (Fig. 1) contains solvent molecules, perchlorate ions and complex cations of composition $[Ln_2(L^{AB4})_3]^{6+}$. In the latter the three ligand strands

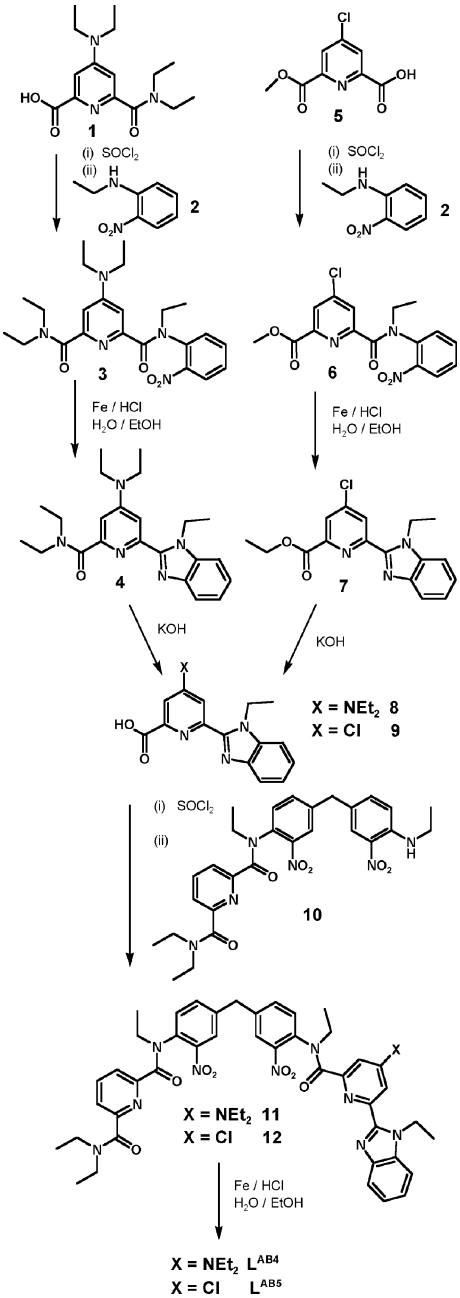

Scheme 3 Synthesis of L^{AB4} and L^{AB5}.

are wrapped tightly around the two lanthanide ions in a helical fashion (Fig. 2 and 3). The complex cations are present in a racemic mixture of *P* and *M* isomers with the helix being either left- or right-handed. The configuration of the ligand strands is HHH meaning that all three carboxamide oxygen atoms are coordinated to the same Ln^{III} ion. It is noteworthy that HHT helicates could not be crystallized with any of the synthesized ligands so far, even with those yielding a high proportion of these isomers in solution. Very weak aromatic stacking interactions contribute to the stability of the complexes. The strongest of these interactions (≈3.5 Å) is between two almost parallel (10–13°) imidazole groups on adjacent ligand strands of the benzimidazole-pyridine-benzimidazole moiety of the ligand (See Tables S3, S4 in the ESI‡ for a full analysis of aromatic interactions). The helical

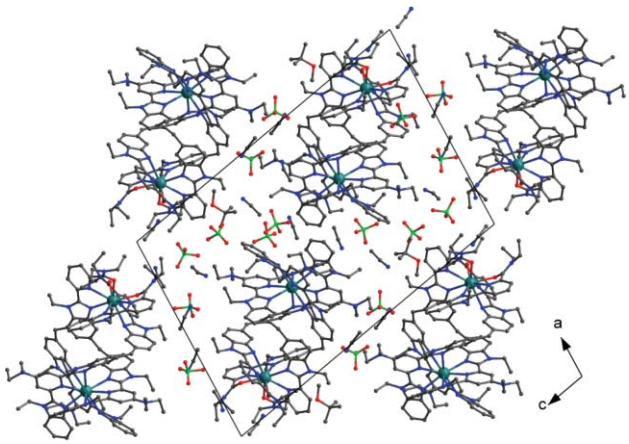

Fig. 1 Cell packing of $[Pr_2(L^{AB4})_3](ClO_4)_6{\cdot}6CH_3CN{\cdot}(CH_3)_3COCH_3$ viewed along the *b* axis.

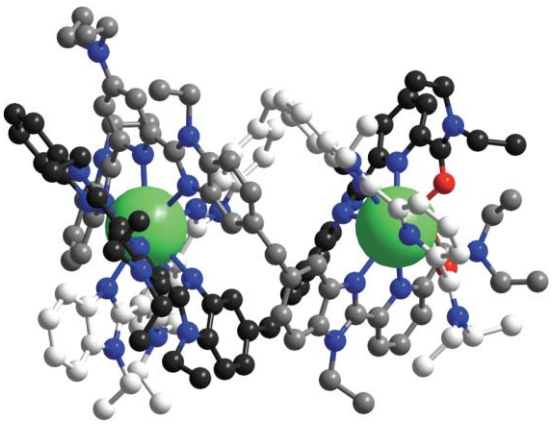

Fig. 2 The $[Pr_2(L^{AB4})_3]^{6+}$ ion in the solid state (Pr green, O red, N blue; C atoms of the three ligand strands are white, grey and black, respectively).

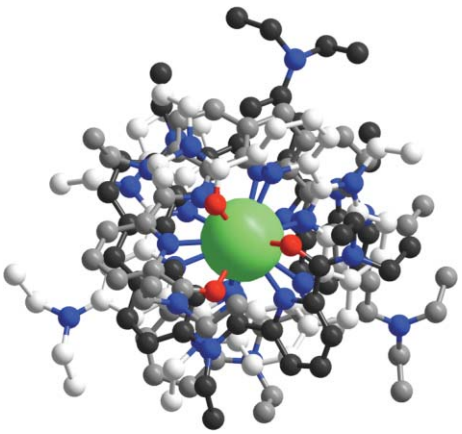

Fig. 3 The $[Pr_2(L^{AB4})_3]^{6+}$ ion viewed along the pseudo C_3 axis. Atom colouring as in Fig. 2.

pitch (the distance for the helix to do a full 360° twist) is 13.3–13.4 Å in the three compounds; the Ln–Ln distance is 9.093–9.156 Å (Table S5, ESI‡). Both of these values are in line with what was found for complexes of L^{AB1} [29] and L^{AB3} [30,37] and do not vary significantly with the size of the Ln^{III} ion or the substituent on the ligands.

The coordination polyhedra around the lanthanide ions can best be described as tricapped trigonal prisms in which bridging benzimidazole nitrogen atoms and either carboxamide oxygen atoms or terminal benzimidazole nitrogen atoms define the upper and lower triangular faces of the prism. Pyridine nitrogen atoms cap the rectangular faces of the prisms (Fig. 4). The most significant deviation from completely regular tricapped trigonal prisms is the twist angle ω of the upper triangular face with respect to the lower triangular face of the prism. In the coordination compartment formed by the benzimidazole-pyridine-carboxamide moieties of the three ligand strands this is found to be 15(3)° for the Pr_2 and Nd_2 complexes and 14(3)° for the Sm_2 complex. In the benzimidazole-pyridine-benzimidazole compartment the angles found for the three complexes are 14(2)°, 13(2)° and 12(1)°, respectively. The values are similar to what has been determined for bimetallic complexes of L^{AB1} [29] and L^{AB3};[30,37] the decrease in twist angle with decreasing ionic radius of the Ln^{III} ion is also typical of this type of complex. A full analysis of the coordination polyhedra including a graphical presentation of the twist angle is given in the ESI‡ (Table S6, Chart S1).

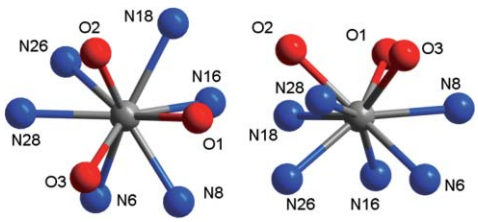

Fig. 4 Two views of the bpa coordination polyhedron in the $[Pr_2(L^{AB4})_3]^{6+}$ ion.

Metal–ligand Ln–X distances are listed in Table 2. Comparing with the distances found in complexes of L^{AB1} [29] and L^{AB3} [30,37] it is concluded that the introduction of a substituent (Cl in L^{AB3}, NEt_2 in L^{AB4}) does not significantly change the Ln–X distances or indeed any other structural parameter measured.

Speciation in CD_3CN solution

Homobimetallic complexes

Reacting two equivalents of $[Ln(ClO_4)_3{\cdot}xH_2O]$ with three equivalents of L^{ABX} in acetonitrile solution gives the corresponding $[Ln_2(L^{ABX})_3](ClO_4)_6$ ($X = 4$ or 5) complexes, which after evaporation of solvent and drying can be dissolved in CD_3CN in preparation for NMR experiments. The spectra contain two sets of signals with different intensities. One set consists of the expected number of signals for a helicate with a set of three equivalent ligand strands; this set of signals is assigned to the HHH-$[Ln_2(L^{ABX})_3]^{6+}$ isomer evidenced in the solid state by X-ray diffraction (Table S7; ESI‡). Diastereotopic methylene protons rule out a linear structure and confirm that the helical structure is maintained in solution. The other set of resonances contains a larger number of signals; overlap of lines and the smaller intensity of this set prevent a full analysis, except in a few cases. An example of this is the 5.2–6.3 ppm range of the spectra of the diamagnetic $[La_2(L^{ABX})_3]^{6+}$, $[Y_2(L^{ABX})_3]^{6+}$ and $[Lu_2(L^{ABX})_3]^{6+}$ homobimetallic helicates (Fig. 5). In the spectra of the free ligands no signals are found in this region, but the helical wrapping of

Table 2 Ln^{III}–X distances in $[Ln_2(L^{AB4})_3](ClO_4)_6 \cdot 6CH_3CN \cdot (CH_3)_3COCH_3$

	Terminal benzimidazole		Bpb unit pyridine		Bridging benzimidazole		Bridging benzimidazole		Bpa unit pyridine		Carboxamide	
Pr_2	N1	2.68(1)	N3	2.58(1)	N4	2.66(1)	N6	2.72(1)	N8	2.59(1)	O1	2.45(1)
	N11	2.65(1)	N13	2.62(1)	N14	2.64(1)	N16	2.63(1)	N18	2.64(1)	O2	2.42(1)
	N21	2.63(1)	N23	2.66(1)	N24	2.69(1)	N26	2.60(1)	N28	2.68(1)	O3	2.416(9)
	Mean	2.65(3)	Mean	2.62(4)	Mean	2.66(3)	Mean	2.65(6)	Mean	2.63(5)	Mean	2.43(2)
Nd_2	N1	2.69(2)	N3	2.56(1)	N4	2.64(2)	N6	2.71(2)	N8	2.62(2)	O1	2.45(1)
	N11	2.67(2)	N13	2.60(1)	N14	2.64(2)	N16	2.67(2)	N18	2.67(1)	O2	2.42(1)
	N21	2.62(2)	N23	2.61(2)	N24	2.68(2)	N26	2.65(2)	N28	2.71(1)	O3	2.44(1)
	Mean	2.66(3)	Mean	2.59(3)	Mean	2.65(2)	Mean	2.67(3)	Mean	2.67(5)	Mean	2.44(2)
Sm_2	N1	2.62(1)	N3	2.53(1)	N4	2.57(1)	N6	2.68(1)	N8	2.53(1)	O1	2.42(1)
	N11	2.63(1)	N13	2.54(1)	N14	2.57(1)	N16	2.59(1)	N18	2.61(1)	O2	2.39(1)
	N21	2.59(1)	N23	2.57(1)	N24	2.65(1)	N26	2.59(1)	N28	2.62(1)	O3	2.37(1)
	Mean	2.61(2)	Mean	2.55(2)	Mean	2.60(5)	Mean	2.62(5)	Mean	2.59(5)	Mean	2.39(3)

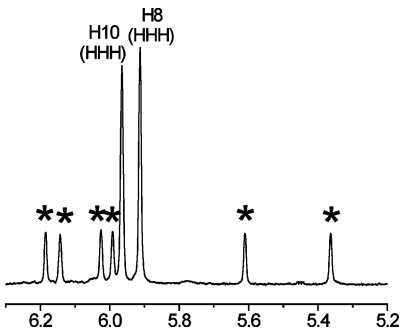

Fig. 5 Partial ^{1}H NMR spectrum of $[La_2(L^{AB5})_3]^{6+}$ in CD_3CN. Signals of the HHT isomer are indicated with *.

the ligand strands brings protons H8 and H10 in the vicinity of aromatic benzimidazole groups of an adjacent ligand strand, causing the signals to be shifted away from their usual location in the spectrum (7.7–7.8 ppm). Apart from the two signals from the three equivalent ligand strands of the HHH isomer, this region contains six additional signals assigned to the H8 and H10 protons of the three non-equivalent ligand strands of the head-head-tail (HHT) isomer in which one ligand strand is oriented in the opposite direction of the other two. Spectra of paramagnetic $[Ln_2(L^{ABX})_3]^{6+}$ complexes (Ln ≠ Y, La, Lu) are less straightforward to interpret since signals are shifted up- or downfield depending on their magnetic interaction with the unpaired electrons of the Ln^{III} ions. Where it is possible to accurately count the number of signals the result is invariably that the less intense set contains approximately three times as many signals as the more intense signal, again leading to the conclusion that the solution contains a mixture of HHH and HHT isomers.

From the integrated intensities of peaks of the two sets of signals the percentages of the two isomers can easily be calculated; the results are given in Table S8 (ESI‡) for complexes of Ln^{III} ions spanning the whole lanthanide series; values for complexes of L^{AB1}, L^{AB2} and L^{AB3} are included for comparison. Two observations are of particular interest here. Firstly, the percentage of HHH isomer is remarkably constant for a given ligand regardless of the Ln^{III} ion (L^{AB1}: 63–73%; L^{AB2}: 6–20%; L^{AB3}: 79–87%; L^{AB4}: 93–96%; L^{AB5}: 53–61%). Secondly, the Cl and NEt_2 substituents have a significant influence on these percentages. For the following discussion of the data, we take the percentages of the HHH-$[Ln_2(L^{AB1})_3]^{6+}$ helicates as a reference. Comparing the weakly electron withdrawing Cl substituent with a Hammett coefficient $\sigma = +0.23$ with the strongly electron donating NEt_2 substituent with $\sigma = -0.73$ (L^{AB2} *vs.* L^{AB3}; L^{AB4} *vs.* L^{AB5}) reveals opposite effects for the two substituents: L^{AB2} lowers HHH yields, while L^{AB3} increases HHH yield. Moreover, the effect is stronger for NEt_2 than for Cl. Finally, a substituent induces the opposite effect when introduced on the bpb instead of the bpa moiety of the ligand (L^{AB2} *vs.* L^{AB4}; L^{AB3} *vs.* L^{AB5}). The yields of HHH complexes thus follow systematically from the sign of the Hammett coefficient of the substituent and the position of the latter on either the bpb or the bpa moiety of the ligand. Remarkably, most percentages deviate from the statistical distribution of 25% HHH and 75% HHT.

Heterobimetallic complexes

CD_3CN solutions for ^{1}H NMR experiments of overall composition $[Ln^1Ln^2(L^{ABX})_3](ClO_4)_6$ ($Ln^1 \neq Ln^2$; $X = 4$ or 5) were obtained like the corresponding homobimetallic complexes from the reaction of one equivalent of each of the lanthanide salts with three equivalents of L^{ABX}. In the stoichiometric solutions of total complex concentration $\approx 10^{-2}$ M the signals observed in the ^{1}H NMR spectra can be attributed to a mixture of different species, all of which are bimetallic triple-stranded complexes composed of two Ln^{III} ions and three ligand strands. Furthermore, the chemical shifts of the protons H8 and H10 confirm that the helical wrapping of the ligands observed in the solid state is maintained in solution. In the diamagnetic complexes the signals of these protons are invariably found in the 5.2–6.3 ppm region, which (as discussed for the homobimetallic complexes) can only be explained by a tight wrapping of the ligand strands around the Ln^{III} ions. In the complexes containing paramagnetic Ln^{III} ions the signals of these protons are shifted considerably, in accordance with their close proximity to the paramagnetic centres. Relevant assignments of the spectra are given in Tables S9 and S10 (ESI‡), while parts of typical spectra are shown on Fig. 6. A complete analysis of the lanthanide induced paramagnetic shifts has also been carried out[39] and will be published separately.

In total, eight different complexes can be formed from the stoichiometric mixture $Ln^1 : Ln^2 : 3L^{ABX}$ (Fig. 7, left). The first

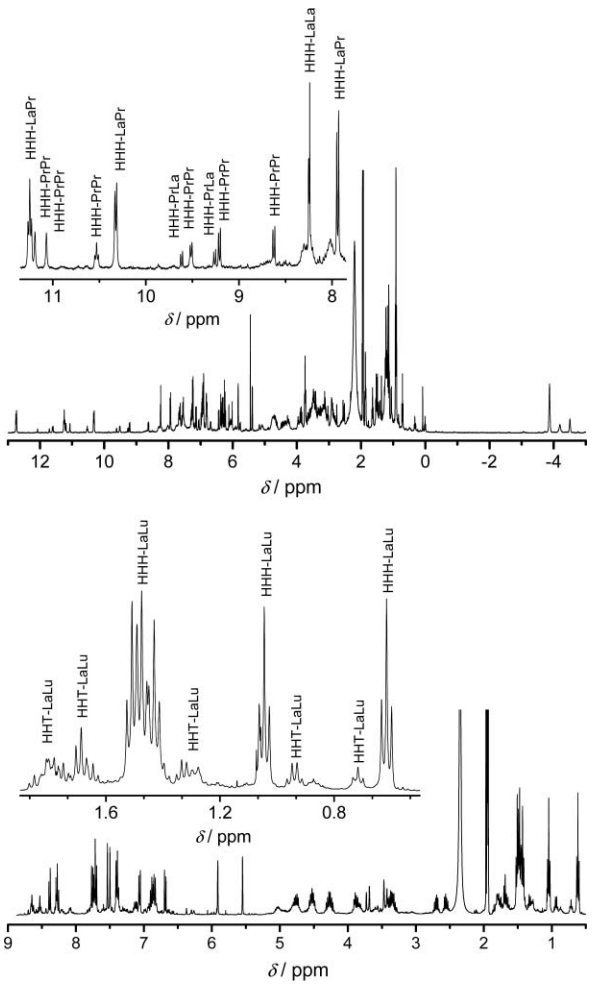

Fig. 6 ^{1}H NMR spectra of mixtures of overall composition La : Pr : 3L^{AB4} (top) and La : Lu : 3L^{AB5} (bottom) with partial assignment used to calculate the percentages of the species in solution.

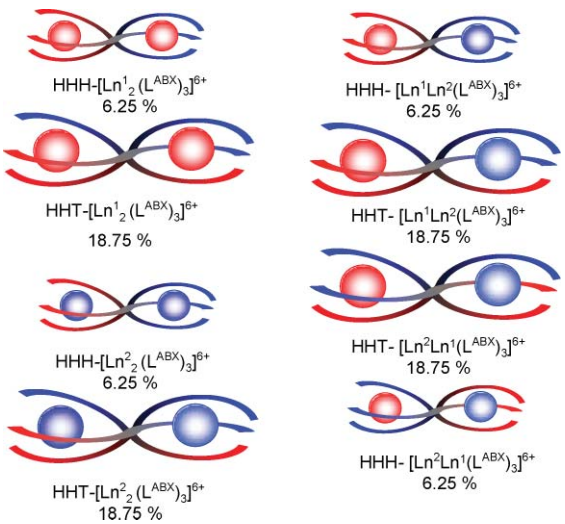

Fig. 7 Schematic representation of the eight possible isomers in a mixture of overall composition Ln^1 : Ln^2 : L^{ABX} = 1 : 1 : 3; the percentages are not meant as predictions of the actual distribution of the species.

four are the HHH and HHT isomers of the homobimetallic complexes containing either two Ln^1 or two Ln^2 ions. For the hetero complexes, the HHH configuration can occur for both [Ln^{1}Ln^2(L^{ABX})$_3$]$^{6+}$ and [Ln^{2}Ln^1(L^{ABX})$_3$]$^{6+}$ complexes; in each case, the Ln^{III} ion mentioned first is in the bpb nonadentate compartment formed by the three ligand strands. By inverting one of the ligand strands, these two helicates give rise to HHT-[Ln^{1}Ln^2(L^{ABX})$_3$]$^{6+}$ and HHT-[Ln^{2}Ln^1(L^{ABX})$_3$]$^{6+}$ isomers, respectively (Fig. 7, right). It should be emphasised that the statistical percentages given in Fig. 7 are not theoretical predictions. Instead, they refer to the hypothetical situation of a heterobitopic ligand exhibiting no inherent selectivity and reacting with a pair of non-distinguishable Ln^{III} ions, far from the present circumstances; these percentages are only included as references for further comparison.

Actually, the speciation of the L^{ABX} complexes departs from the hypothetical statistical distribution in a remarkable manner (Fig. 8; Tables S11, S12, and S13; ESI‡). For L^{AB1} the percentage of hetero complexes varies from ≈50% for neighbouring pairs of lanthanide ions to ≈95% for the La/Lu pair. Furthermore, the relative percentages of HHH and HHT are far from statistical; no HHT isomers of hetero complexes have been observed. Finally, of the two possible HHH hetero complexes, the only isomer usually observed is the one with the larger Ln^{III} ion in the bpb compartment of the helicate. Exceptions occur when the pair of lanthanide ions have very similar sizes, but even for the adjacent La^{III}/Ce^{III} pair, the HHH-[LaCe(L^{AB1})$_3$]$^{6+}$ isomer largely dominates over the HHH-[CeLa(L^{AB1})$_3$]$^{6+}$ helicate. In the ligand design for L^{ABX} (X = 2–5), introduction of an electron donating NEt$_2$ group on the bpa moiety of L^{AB2} and of a electron withdrawing Cl substituent on the bpb moiety of L^{AB5} was expected to modify the electron density of the corresponding pyridine nitrogen donor atom and improve the yield of hetero complexes. With the same reasoning, the yield of the hetero species was predicted to decrease with ligands L^{AB3} and L^{AB4} in which the same two substituents are introduced on the opposite moieties of the ligands. As can be seen from Fig. 8 in which the percentages of the heterobimetallic species are plotted against the differences in ionic radii Δr_i, no important improvement in the yield of the hetero species compared to L^{AB1} is observed for any of the four substituted ligands. The behaviour of the three ligands L^{ABX} (X = 3–5) deviates somewhat compared to L^{AB1}, but the general trend

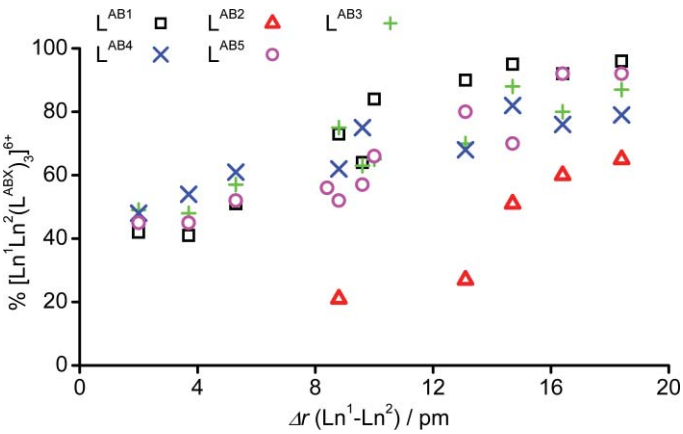

Fig. 8 Percentages of heterobimetallic [Ln^{1}Ln^2(L^{ABX})$_3$]$^{6+}$ complexes in CD$_3$CN.

is maintained, in that selectivity increases with Δr_i. While keeping up with this trend, L^{AB2} displays a markedly different behaviour in that the concentration of the hetero species remains very low (20–65%). Differences between the four ligands with $X = 1$, 3, 4 and 5 are maximum for $\Delta r_i \approx 8$–15 pm and minimum for both smaller and larger values of Δr_i.

This unexpected behaviour can be explained with reference to the concentrations of the HHH isomer determined for the homobimetallic helicates. Indeed, for a large selectivity of the ligand towards a heteropair of lanthanide ions, it is important that the ligand has a tendency to organise in the HHH configuration, which is consistent with the non-observation of HHT isomers for heterobimetallic helicates. Both ligands (L^{AB2} and L^{AB5}) expected to give improved yields of hetero complexes compared to L^{AB1} eventually gave lower yields. L^{AB2} forms very low HHH yields of homobimetallic helicates (6–20%) compared to 63–73% for L^{AB1}, while L^{AB5} induces only slightly smaller yields (53–61%). Concomitantly, the La/Lu solution with L^{AB2} contains only 65% of the heterobimetallic species, as compared to 96% for L^{AB1} and 92% for L^{AB5}. On the other hand, an opposite behaviour is observed for L^{AB3} (79–87% of HHH homobimetallic isomer) and L^{AB4} which leads almost exclusively to the HHH isomers (93–96%). While the former ligand results in concentrations of hetero species consistent with the proportion of HHH isomers (*e.g.* 87% for the La/Lu pair), L^{AB4} deviates from expectations. It is only slightly more selective than L^{AB1} for $\Delta r_i \approx 2$–5 pm and less for $\Delta r_i > \approx 5$ pm: the proportion of hetero helicate amounts to only 79% for the La/Lu pair. The results obtained for L^{AB3} and L^{AB4} confirm that the ligand design strategy is well-founded in the sense that these two ligands as predicted give lower yields of heterobimetallic complexes, despite higher HHH yields.

Conclusions

The effect of electron donating and electron withdrawing substituents grafted on the pyridine of the bpb tridentate coordination unit of L^{AB1} have been compared to those induced by similar substitutions of the bpa coordination site.[30] The resultant modification of the electron density of the pyridine N-donor atoms induces systematic effects on the proportions of HHH isomers in the homobimetallic solutions and of hetero helicates in Ln^1/Ln^2 heterobimetallic solutions for ligands L^{AB2}, L^{AB3}, and L^{AB4}, compared to L^{AB1}. The main factor here is the difference in coordination strength of the two tridentate coordination units. We have shown previously that if this difference is too large, a large proportion of HHT isomer occurs, detrimental to the selectivity for a hetero pair of lanthanide ions.[29] The two substituents chosen for this study have weak effects, in line with the very small energy difference between HHT and HHH isomers ($\Delta G° \approx 0$–7 kJ mol^{-1}).[37] Since the bpb coordinating unit is less coordinating than the bpa unit, it is more affected by the substitution, particularly by NEt_2. In fact, L^{AB4} was predicted to yield less HHH isomers since the coordination strength between the two coordinating units is more equalized. This is by far not the case, but we note that due to less difference in the coordination ability of the bpb and bpa units, the proportion of the Ln^2Ln^1 isomer (with respect to Ln^1Ln^2) is twice as large for L^{AB4}, compared to L^{AB5} for $\Delta r_i < 5.3$ pm. This shows how the self-assembly of supramolecular structures depends on subtle effects. Some of them can be fine-tuned in a predictable and conceptually straightforward manner, while others still escape complete control. However, progress in the understanding of the factors leading to the stability of helical polymetallic assemblies in solution,[40,41] particularly of the weaker interactions contributing to the stability of supramolecular edifices, should soon lead to improved handling of these problems.

Acknowledgements

This project is supported through grants from the Swiss National Science Foundation.

References

1 J.-C. G. Bünzli and C. Piguet, *Chem. Soc. Rev.*, 2005, **34**, 1048–1077.
2 S. Comby and J.-C. G. Bünzli, in *Handbook on the Physics and Chemistry of Rare Earths*, ed. K. A. Gscheidner, Jr., J.-C. G. Bünzli and V. K. Pecharsky, Elsevier Science B. V., Amsterdam, 2007, vol. 37.
3 I. Hemmilä and V. Laitala, *J. Fluoresc.*, 2005, **15**, 529–542.
4 K. Nishioka, K. Fukui and K. Matsumoto, in *Handbook on the Physics and Chemistry of Rare Earths*, ed. K. A. Gscheidner, Jr., J.-C. G. Bünzli and V. K. Pecharsky, Elsevier Science B. V., Amsterdam, 2007, vol. 37.
5 S. Pandya, J. Yu and D. Parker, *Dalton Trans.*, 2006, 2757–2766.
6 R. J. Aarons, J. K. Notta, M. M. Meloni, J. Feng, R. Vidyasagar, J. Narvainen, S. Allan, N. Spencer, R. A. Kauppinen, J. S. Snaith and S. Faulkner, *Chem. Commun.*, 2006, 909–911.
7 M. M. Hüber, A. B. Staubli, K. Kustedjo, M. H. B. Gray, J. Shih, S. E. Fraser, R. E. Jacobs and T. J. Meade, *Bioconjugate Chem.*, 1998, **9**, 242–249.
8 H. C. Manning, T. Goebel, R. C. Thompson, R. R. Price, H. Lee and D. J. Bornhop, *Bioconjugate Chem.*, 2004, **15**, 1488–1495.
9 I. Nasso, C. Galaup, F. Havas, P. Tisnès, C. Picard, S. Laurent, L. Vander Elst and R. N. Muller, *Inorg. Chem.*, 2005, **44**, 8293–8305.
10 C. Picard, N. Geum, I. Nasso, B. Mestre, P. Tisnès, S. Laurent, R. N. Muller and L. Vander Elst, *Bioorg. Med. Chem. Lett.*, 2006, **16**, 5309–5312.
11 Q. Zheng, H. Dai, M. E. Merritt, C. Malloy, C. Y. Pan and W.-H. Li, *J. Am. Chem. Soc.*, 2005, **127**, 16178–16188.
12 L. J. Martin, M. J. Hähnke, M. Nitz, J. Wöhnert, N. R. Silvaggi, K. N. Allen, H. Schwalbe and B. Imperiali, *J. Am. Chem. Soc.*, 2007, **129**, 7106–7113.
13 J.-P. Costes, F. Dahan, A. Dupuis, S. Lagrave and J.-P. Laurent, *Inorg. Chem.*, 1998, **37**, 153–155.
14 J. W. Buchler, A. de Cian, J. Fischer, M. Kihn-Botulinski and R. Weiss, *Inorg. Chem.*, 1988, **27**, 339–345.
15 N. Ishikawa, T. Iino and Y. Kaizu, *J. Am. Chem. Soc.*, 2002, **124**, 11440–11447.
16 V. Jacques and J. F. Desreux, *Top. Curr. Chem.*, 2002, **221**, 123–164.
17 G. Bernardinelli, C. Piguet and A. F. Williams, *Angew. Chem., Int. Ed. Engl.*, 1992, **31**, 1622–1624.
18 C. Piguet, J.-C. G. Bünzli, G. Bernardinelli, G. Hopfgartner and A. F. Williams, *J. Am. Chem. Soc.*, 1993, **115**, 8197–8206.
19 N. Martin, J.-C. G. Bünzli, V. McKee, C. Piguet and G. Hopfgartner, *Inorg. Chem.*, 1998, **37**, 577–589.
20 M. Elhabiri, R. Scopelliti, J.-C. G. Bünzli and C. Piguet, *J. Am. Chem. Soc.*, 1999, **121**, 10747–10762.
21 C. P. Iglesias, M. Elhabiri, M. Hollenstein, J.-C. G. Bünzli and C. Piguet, *J. Chem. Soc., Dalton Trans.*, 2000, 2031–2043.
22 R. Tripier, M. Hollenstein, M. Elhabiri, A.-S. Chauvin, G. Zucchi, C. Piguet and J.-C. G. Bünzli, *Helv. Chim. Acta*, 2002, **85**, 1915–1929.
23 C. D. B. Vandevyver, A.-S. Chauvin, S. Comby and J.-C. G. Bünzli, *Chem. Commun.*, 2007, 1716–1718.
24 A.-S. Chauvin, S. Comby, B. Song, C. D. B. Vandevyver, F. Thomas and J.-C. G. Bünzli, *Chem.–Eur. J.*, 2007, **13**(34), 9515–9526.
25 S. Floquet, N. Ouali, B. Bocquet, G. Bernardinelli, D. Imbert, J.-C. G. Bünzli, G. Hopfgartner and C. Piguet, *Chem.–Eur. J.*, 2003, **9**, 1860–1875.
26 K. Zeckert, J. Hamacek, J.-M. Senegas, N. Dalla-Favera, S. Floquet, G. Bernardinelli and C. Piguet, *Angew. Chem., Int. Ed.*, 2005, **44**, 7954–7958.

27 S. Petoud, J.-C. G. Bünzli, F. Renaud, C. Piguet, K. J. Schenk and G. Hopfgartner, *Inorg. Chem.*, 1997, **36**, 5750–5760.
28 T. Le Borgne, P. Altmann, N. André, J.-C. G. Bünzli, G. Bernadinelli, P.-Y. Morgantini, J. Weber and C. Piguet, *Dalton Trans.*, 2004, 723–733.
29 N. André, T. B. Jensen, R. Scopelliti, D. Imbert, M. Elhabiri, G. Hopfgartner, C. Piguet and J.-C. G. Bünzli, *Inorg. Chem.*, 2004, **43**, 515–529.
30 T. B. Jensen, R. Scopelliti and J.-C. G. Bünzli, *Inorg. Chem.*, 2006, **45**, 7806–7814, (*Inorg. Chem.*, 2007, **46**, 1507).
31 B. Lamm, *Acta Chem. Scand.*, 1965, **19**, 2316–2322.
32 J. F. Desreux, in *Lanthanide Probes in Life, Chemical and Earth Sciences. Theory and Practice*, ed. J.-C. G. Bünzli and G. R. Choppin, Elsevier Science Publ. B. V., Amsterdam, The Netherlands, 1989.
33 W. C. Wosley, *J. Chem. Educ.*, 1973, **50**, A335.
34 K. N. Raymond, *Chem. Eng. News*, 1983, **Dec 12**, 2.
35 *CrysAlis RED Version 1.7.0*, Oxford Diffraction Ltd., Abingdon, OX14 4RX, Oxfordshire, UK2003.
36 *SHELXTL Release 5.1*, Bruker AXS, Madison, WI 53719, USA, 1997.
37 T. B. Jensen, R. Scopelliti and J.-C. G. Bünzli, *Chem.–Eur. J.*, 2007, **13**, 8404–8410.
38 M. A. Phillips, *J. Chem. Soc.*, 1928, 172–177.
39 T. B. Jensen, PhD thesis, École Polytechnique Fédérale de Lausanne (EPFL), 2006.
40 G. Canard and C. Piguet, *Inorg. Chem.*, 2007, **46**, 3511–3522.
41 J. Hamacek, M. Borkovec and C. Piguet, *Dalton Trans.*, 2006, 1473–1490.

